Tranilast inhibits the growth and metastasis of mammary carcinoma

Rabindranath Chakrabarti[a], Venkateswaran Subramaniam[a], Salma Abdalla[a], Serge Jothy[a,b] and Gérald J. Prud'homme[a,b]

Tranilast (*N*-[3,4-dimethoxycinnamonyl]-anthranilic acid) is a drug of low toxicity that is orally administered, and has been used clinically in Japan as an antiallergic and antifibrotic agent. Its antifibrotic effect is thought to depend on the inhibition of transforming growth factor-beta (TGF-β). It has also been shown to exert antitumor effects, but its mode of action is unclear. Here, we explored the antitumor effects of tranilast *in vitro* and *in vivo*. Tranilast inhibited the proliferation of several tumor cell lines including mouse mammary carcinoma (4T1), rat mammary carcinoma stem cell (LA7), and human breast carcinoma (MDA-MB-231 and MCF-7). Tranilast blocked cell-cycle progression *in vitro*. In the highly metastatic 4T1 cell line, tranilast inhibited phospho-Smad2 generation, consistent with a blockade of TGF-β signaling. It also inhibited the activation of MAP kinases (extracellularly regulated kinase 1 and 2 and JNK), which have been linked to TGF-β-dependent epithelial-to-mesenchymal transition and, indeed, it blocked epithelial-to-mesenchymal transition. Although tranilast only partially inhibited TGF-β production by 4T1 tumor cells, it potently inhibited the production of TGF-β, interferon-γ, IL-6, IL-10, and IL-17 by lymphoid cells, suggesting a general anti-inflammatory activity. *In vivo*, female BALB/c mice were inoculated with syngeneic 4T1 cells in mammary fat pads and treated with tranilast by gavage. Tranilast reduced (>50%) the growth of the primary tumor. However, its effects on metastasis were more striking, with more than 90% reduction of metastases in the lungs and no metastasis in the liver. Thus, tranilast has potential activity as an antimetastatic agent in breast cancer. *Anti-Cancer Drugs* 20:334–345 © 2009 Wolters Kluwer Health | Lippincott Williams & Wilkins.

Anti-Cancer Drugs 2009, **20**:334–345

Keywords: breast cancer, extracellularly regulated kinase 1 and 2, mammary carcinoma, metastasis, tranilast, transforming growth factor-beta

[a]Department of Laboratory Medicine and Li Ka Shing Knowledge Institute, St Michael's Hospital and [b]Department of Laboratory Medicine and Pathobiology, University of Toronto, Toronto, Ontario, Canada

Correspondence to Gérald J. Prud'homme, MD, Department of Laboratory Medicine, St Michael's Hospital and University of Toronto, 30 Bond Street, Toronto, Ontario, Canada M5B 1W8
Tel: +416 864 6060 x3147; fax: +416 864 5648;
e-mail: prudhommeg@smh.toronto.on.ca

Received 3 December 2008 **Revised form accepted** 23 December 2008

Introduction

Breast cancer is a leading cause of death in women [1]. Advances in screening, diagnosis, and anticancer therapy have increased survival. However, there are still many cases where the tumor metastasizes to bones, lungs, and liver, causing debilitating disease and death. Current therapies have a limited impact at this stage, and there is an urgent need to develop new therapies.

Tranilast (*N*-[3,4-dimethoxycinnamonyl]-anthranilic acid) is an orally active compound used clinically in Japan to control allergic responses such as anaphylactic reactions, atopic dermatitis, and allergic rhinitis, where it seems to act on mast cells [2–5]. Tranilast also inhibits collagen synthesis and fibroblast proliferation, and has been used to control fibrotic disorders [3,6–9]. Although the mechanism(s) of this antifibrotic effect are not fully elucidated, it is thought that the inhibition of transforming growth factor-beta (TGF-β) production or action is a key factor [3,6,8,9–14].

In addition, tranilast has been shown to exert antiproliferative and/or antitumor protective effects against glioma cells, uterine leiomyoma cells, oral squamous cell carcinoma, and pancreatic carcinoma [15–18]. In some of these studies, there is also evidence that the inhibition of TGF-β is involved, although the mechanisms of action remain unclear. In the case of mouse mammary or human breast carcinoma, TGF-β1 appears to be a particularly important factor in the development of metastases [19–24]. Therefore, we hypothesized that tranilast would protect against the development of these metastases.

In this study, we examined the inhibitory effects of tranilast against breast or other cancer cell lines, and particularly the highly metastatic 4T1 mouse mammary carcinoma cell line. We found that tranilast inhibited the proliferation of all the cell lines tested, TGF-β-induced Smad phosphorylation and other signaling pathways, and epithelial-to-mesenchymal transition (EMT). It also exerted a broad suppressive effect on immune cells. Most importantly, it inhibited the growth and metastatis of the 4T1 cell line (>90% reduction of metastases). These findings are of special interest because, clinically, tranilast has few adverse effects, as compared with conventional

0959-4973 © 2009 Wolters Kluwer Health | Lippincott Williams & Wilkins DOI: 10.1097/CAD.0b013e328327994e

anticancer drugs, and might find a new application in the prevention of metastatic breast cancer.

Materials and methods

Cancer cell lines and reagents

All the cancer cell lines were obtained from ATCC (Manassas, Virginia, USA). 4T1 is an estrogen-independent mammary carcinoma, derived from mammary epithelial carcinoma from BALB/c mice (BALB/cfC3H). 4T1-derived tumors mimic clinical breast cancer and are highly metastatic [25]. MCF-7 and MDA-MB-231 are breast carcinoma cells of human origin. LA7 is a mammary tumor cell line derived from a Sprague–Dawley rat, which has recently been found to have mammary cancer stem cell properties [26]. Lewis lung carcinoma (LLC) is a murine lung carcinoma derived from a C57BL/6 mouse. EL4 is a mouse T lymphoma cell line established from a lymphoma induced in a C57BL/6 mouse by 9,10-dimethyl-1,2-benzanthracene. Unless otherwise mentioned, cells were grown in Dulbecco's Modified Eagle Medium supplemented with 10% fetal bovine serum and antibiotics (complete medium). Tranilast was a gift from Dr Richard Gilbert (St Michael's Hospital, Toronto, Canada). Propidium iodide and DNase-free RNase A were from Sigma-Aldrich, Missouri, USA.

Animal experiments

All animal experiments were performed according to the guidelines of the Canadian Council on Animal Care's Ethics of Animal Investigation. The 4T1 cells were transplanted orthotopically in mammary fat pads (5×10^5 cells/pad/mouse in 50 µl) of 6-week-old syngeneic BALB/c mice (Charles River Laboratories, Wilmington, Massachusetts, USA) under anesthesia. Mice were given tranilast or vehicle by daily gavage at a dose of 300 mg/kg body weight from day 0 (day of cancer cell transplantation) to the end of the treatment. Tranilast was dissolved in 1% $NaHCO_3$ for this purpose. Neutralized 1% $NaHCO_3$ served as the vehicle. Tumor growth was measured by caliper in two dimensions, and the volumes were calculated using the formula $(\text{width}^2 \times \text{length})/2$. On day 28 of treatment the mice were killed and organs were collected.

Histology and histomorphometry

The tissues were fixed in 10% neutral buffered formalin for 24 h. Paraffin sections were made and the tissue sections were stained with eosin and hematoxylin. Metastatic disease was quantified by counting the number of metastatic tumor foci per lung and liver section. For morphometry, the pictures were taken at $\times 4$ magnification and the area of each metastatic tumor lesion was measured in each lung section by a morphometric method (ImageJ software from NIH, Bethesda, Maryland, USA). The mean area per metastatic tumor in each lung section was calculated.

Epithelial-to-mesenchymal transition

4T1 cells were grown in 24-well plates containing round cover slips. Covers slips with attached cells were transferred to new wells containing TGF-β1, tranilast, or both and cultured for 48 h. After that, cells were washed twice with phosphate-buffered saline (PBS), fixed with 3.7% formaldehyde solution in PBS for 10 min at room temperature. Cells were washed and permeabilized with 0.1% Triton X-100 for 5 min, washed and incubated with PBS containing 1% bovine serum albumin for 20 min at room temperature. Alexa Fluor 568-conjugated phalloidin (Molecular Probes, Eugene, USA) was added to the cells (40x dilutions final) and incubated for another 20 min. Cells were washed, air dried, mounted on the slide, examined under florescence microscope (Olympus BX50, Model F4, Olympus Optical Co. Ltd, Shinjuku-ku, Tokyo, Japan) and photomicrographs were taken at a magnification of $\times 400$.

Immunofluorescence staining for phosphorylated Smad2

4T1 cells were allowed to adhere directly to the microscopic slides. For phosphorylated Smad2 (pSMAD2) expression, TGF-β1, tranilast or both added to the cells attached to the slides and incubated for 20 h. Cells were stained for nuclear pSmad2 with anti-pSmad2 antibody (Catalog # AB3849, Chemichon International, Temecula, California, USA). Anti-rabbit IgG-fluorescein isothiocyanate (Catalog # F-1268, Sigma-Aldrich, St Louis, Missouri, USA) was used as the secondary antibody. Cells were fixed and permeabilized using a cell fixation/permeabilization kit (Becton Dickinson, Mississauga, Ontario, Canada). In brief, cells were washed with PBS containing 1% bovine serum albumin, fixed and permeabilized with cytofix/cytoperm solution for 20 min at 4°C, washed with perm/wash buffer, incubated with primary antibodies for 1 h at 4°C, washed, incubated with fluorescein isothiocyanate-conjugated secondary antibody for 1 h at 4°C, washed and mounted. The stained cells were examined under a fluorescence microscope (Olympus BX50) and photographs taken.

Western blot analysis

For the detection of pSmad2 and vimentin, the appropriately treated cell cultures (4T1) were lysed in buffer (50 mmol/l Tris pH 7.6, 150 mmol/l NaCl, 0.1% NP-40) containing the cocktail of protease inhibitors (PMSF, leupeptin, pepstatin, and aprotinin) on ice. Concentrated (5x) Laemmli sodium dodecyl sulfate sample buffer containing β-mercaptoethanol was added to the cell lysates and incubated for 5 min in a boiling water bath, vortexed and appropriate amount loaded onto a 12% sodium dodecyl sulfate-polyacrylamide gel electrophoresis for western blot analysis with appropriate primary antibodies – rabbit anti-Smad2 phosphorylated antibody (Catalog # AB3849, Chemicon International, USA), rabbit anti-TGF-β (Catalog # 3709, Cell Signaling, Boston, Massachusetts, USA) and rabbit anti-vimentin (Catalog # sc-5565, Santa Cruz biotechnology, Santa

Cruz, California, USA). The secondary antibody was goat anti-rabbit horseradish peroxidase (Catalog # W4011, Promega, Madison, Wisconsin, USA).

Effect of tranilast on the growth of tumor cells in culture

All the tumor cells (10×10^3/well) were allowed to attach to the wells of flat bottom 96-well plate. Various concentrations of tranilast [dissolved in dimethyl sulfoxide (DMSO)] or DMSO were added to the cells and cultured for 48 h. Cell growth was measured by MTT assay. In brief, MTT was added to the cells at 1 mg/ml final concentration and incubated for 2 h. Supernatant was removed, formazan solubilized with isopropanol, and absorbance read at a wavelength of 540 nm.

Flow cytometry for cell-cycle analysis and annexin V staining

The 4T1 cells were harvested by trypsinization, washed with PBS, and fixed in cold 70% ethanol for 3 h and stored at -20°C. For staining with propidium iodide, ethanol was removed by centrifugation followed by a wash in PBS. The cell pellets were resuspended in 1 ml staining solution (PBS containing 0.1% Triton X-100, 50 μg/ml propidium iodide and 50 U/ml of DNase-free RNase A) and incubated at room temperature for 30 min. After that, cell cycle was analyzed by flow cytometry using the program FlowJO (Tree Start Inc., Eugene, Oregon, USA). Annexin V staining of tumor cells for the detection of apoptosis was performed with a commercial kit (Clontech, Mountain View, California, USA), and analyzed by flow cytometry, according to the manufacturer's instructions.

Determination of extracellularly regulated kinase 1 and 2 and JNK phosphorylation by CASE ELISA

The 4T1 cells (10×10^3/well) were grown on a flat-bottom 96-well plate overnight, followed by serum deprivation for 24 h. Then the cells were cultured for another 20 h in complete medium with or without tranilast. The level of phosphorylated and total extracellularly regulated kinase 1 and 2 (ERK1/2) and JNK were measured by enzyme-linked immunosorbent assay (ELISA) using cellular activation of signaling ELISA (CASE) kits (SuperArray Bioscience Corp., Frederick, Maryland, USA). The extent of protein phosphorylation was determined according to the supplier's protocol.

Lymphocyte culture and stimulation

Spleen cell isolation, splenic T cell purification, culture conditions, stimulation with CD3/CD28 mAbs or lipopolysaccharide (LPS) was performed as we have described earlier [27–29].

Cytokine enzyme-linked immunosorbent assay

Cytokine levels (IL-6, IL-10, interferon-γ, IL-17, and TGF-β1) in the culture supernatants were measured by specific ELISA kits (R&D Systems, Minneapolis, Minnesota, USA), according to the supplier's protocol. For TGF-β1 measurement, the samples were acidified for the activation of the cytokine followed by neutralization, according to the supplier's protocol. The TGF-β1 assay detects only the active form of the cytokine.

Statistical analysis

Significance of difference between treated and untreated groups were analyzed by two-tailed *t*-test, and $P \leq 0.05$ was considered significant. All analyses were performed with GraphPad Prism 3.03 (GraphPad Software, La Jolla, California, USA).

Results

Tranilast inhibits the growth of tumor cells *in vitro*

We examined whether tranilast has a growth inhibitory effect on tumor cells *in vitro*. As shown in Fig. 1a, tranilast markedly inhibited the growth of 4T1 cells, with 50 and 100% inhibition at 200 and 800 μmol/l, respectively. DMSO, the solvent for tranilast, did not show any inhibitory effect on the growth up to the maximum dose used (0.8% for 800 μmol/l tranilast) (data not shown). At these doses of tranilast, no increase in cell death was noted as determined by the Trypan blue dye exclusion, and there was no increase in apoptosis as determined by flow cytometric analysis of annexin V staining (data not shown). Tranilast also inhibited the growth of several other cancer cell lines (Fig. 1a), including human breast carcinoma lines (MDA-MB-231 and MCF-7), mouse LLC, and mouse thymoma (EL4). The most sensitive cell line was rat mammary carcinoma LA7, which has stem cell properties [26], showing 50% inhibition at 100 μmol/l.

Tranilast arrests cell-cycle progression in 4T1 cells

We further examined the effect of tranilast on the cell cycle. As shown in Fig. 1b, at 800 μmol/l tranilast, the number of G_1 cells increased (58%) with concomitant decrease in G_2 cells (0.5%), without any changes in S-phase cell number (40%), as compared with the controls ($G_1 = 43\%$, $S = 40\%$, $G_2 = 16\%$). Thus, the cell cycle seemed to be arrested at the G_1 phase. In addition, Ki-67 nuclear staining by immunofluorescence was restricted to a few foci in the nucleoplasm, which is also indicative of G_1-phase arrest [30] (data not shown). However, at a lower concentration of tranilast (200 μmol/l), the number of S-phase cells increased (72%) with concomitant decrease in G_1 (17%) and G_2 (8%) cell numbers, as compared with the control (Fig. 1b), indicating an inhibition of cell-cycle progression at the S-phase. In summary, these results indicate that tranilast can arrest the cell cycle at either the G_1 or S-phase, depending on the drug concentration.

Tranilast inhibits phosphorylated Smad2 accumulation in the nucleus

Phosphorylation of Smad2 and the translocation of pSmad2 to the nucleus are key events in the TGF-β1 signal transduction cascade [31]. We examined the effect

Fig. 1

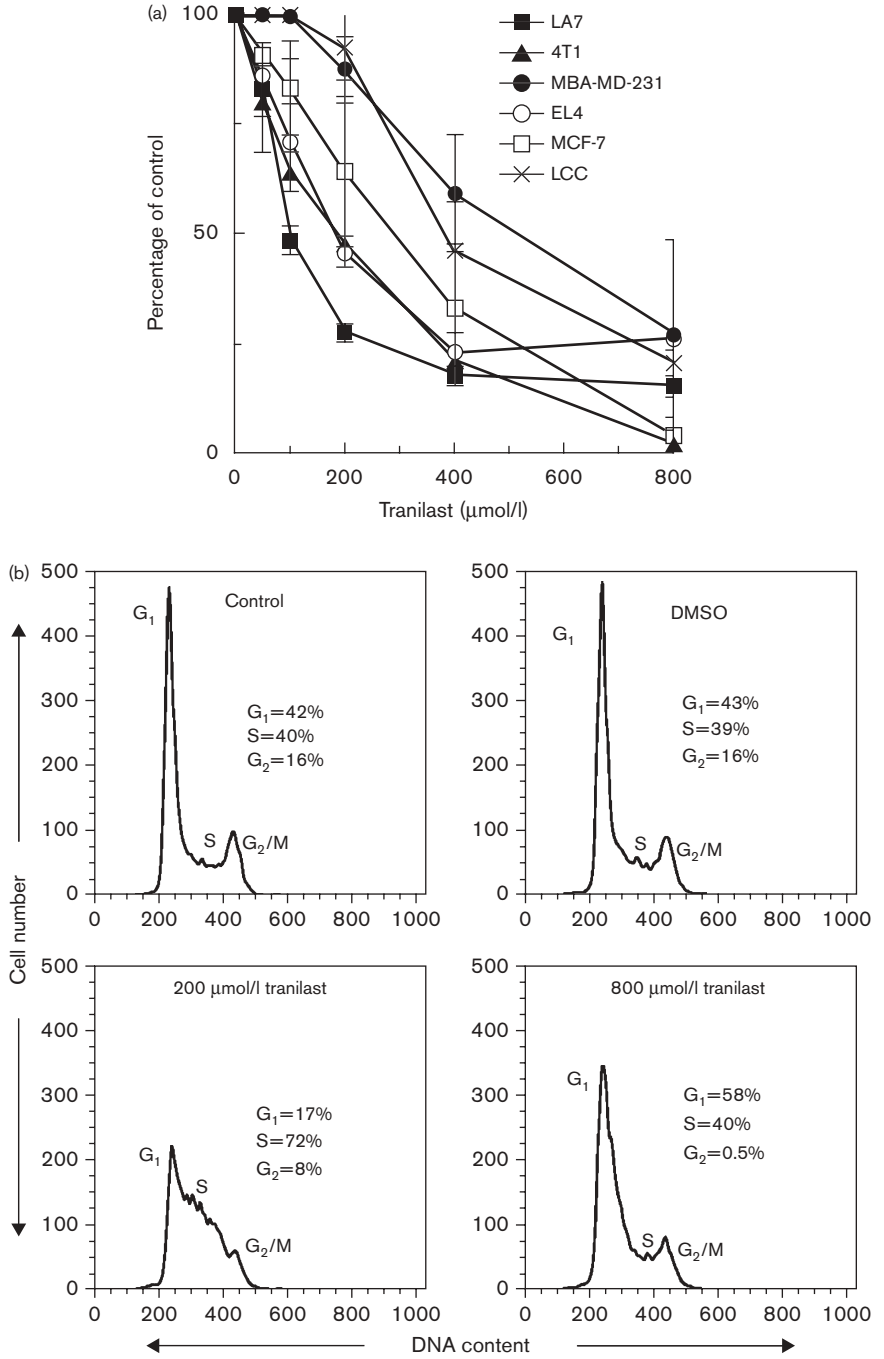

Effect of tranilast on the growth of breast cancer and other tumor cell lines *in vitro*. (a) Various tumor cells (LA7, 4T1, MDA-MB-231, LLC, EL4, MCF-7 cells) were allowed to attach to the wells (10×10^3 cells/well) of a flat-bottom 96-well plate. Various concentrations of tranilast were added to the cells and cultured for 48 h. Cell growth was monitored by MTT assay. Growth or proliferation in all cell lines was suppressed, with LA7 being the most sensitive. The suppression of cell growth was not accompanied by cytotoxicity (data not shown). Results are the mean ± SD of three separate experiments. (b) 4T1 cells were cultured for 24 h in serum-free medium, followed by the culture in complete medium in the presence or absence of dimethyl sulfoxide (DMSO) or tranilast for 24 h. Then cell-cycle progression was analyzed by flow cytometry. The percentage of cells in the G_1, S, or G_2 phases is reported inside each histogram. Tranilast inhibited cells cycle in the S-phase at 200 μmol/l, and primarily at the G_1 phase at 800 μmol/l. Two experiments yielded similar results.

of tranilast on the nuclear accumulation pSmad2 in 4T1 cells treated with active TGF-β1. Control cells (not treated with TGF-β1) showed the presence of some pSmad2 in the nucleus (Fig. 2a), consistent with our finding that this cell line produces TGF-β1. The levels of TGF-β1 in the culture supernatants at 0, 50, 200, and

Fig. 2

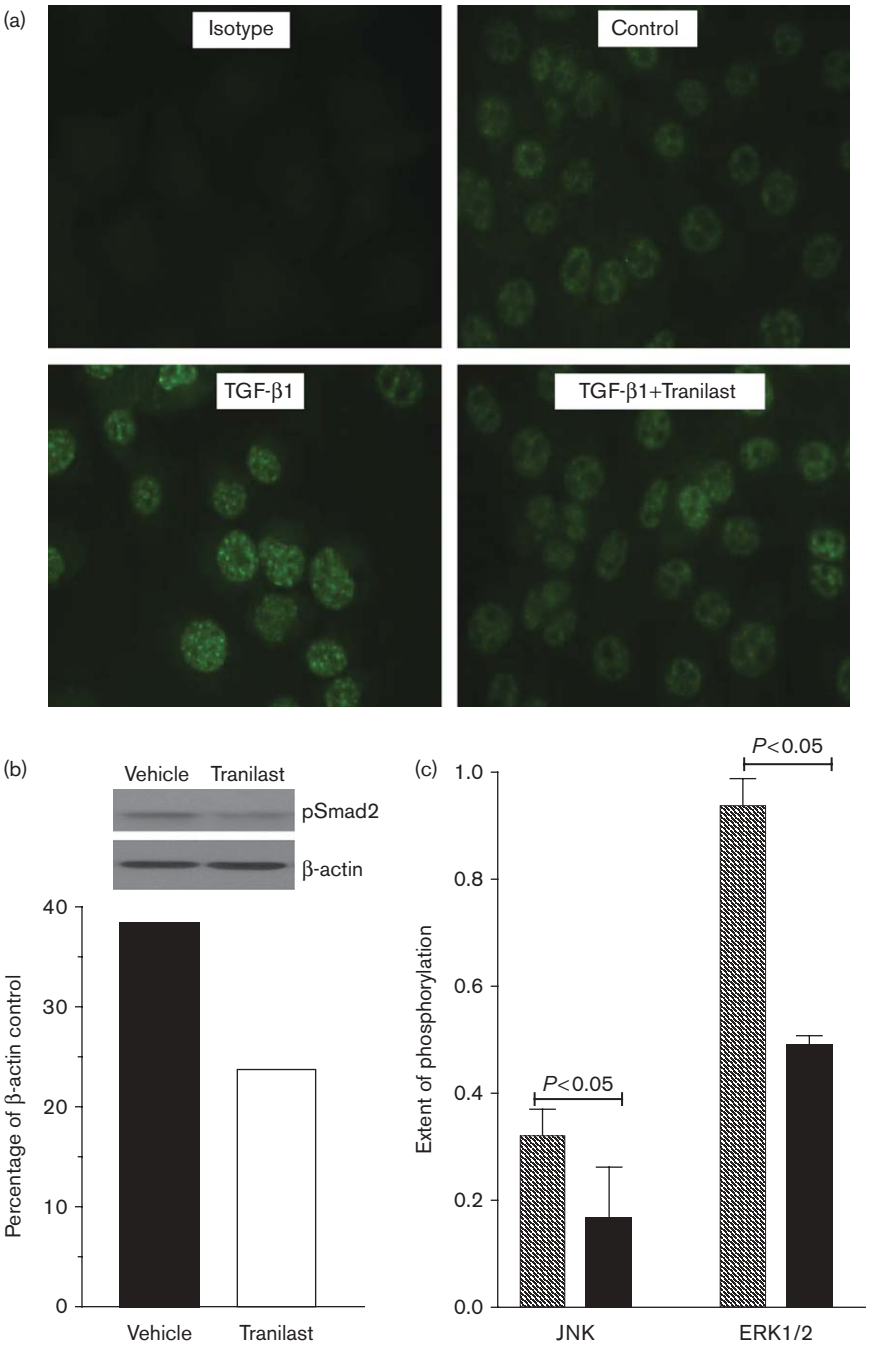

Tranilast inhibits TGF-β1-induced Smad2 phosphorylation and serum-induced extracellularly regulated kinase 1 and 2 (ERK1/2) phosphorylation in 4T1 cells. (a) 4T1 cells were attached directly to microscopic slides and incubated for 20 h in the presence of TGF-β1 (2 ng/ml), tranilast (800 μmol/l), or both, and stained for phosphorylated Smad2 (pSmad2) as described in Materials and methods. The cells receiving only vehicle [dimethyl sulfoxide (DMSO)] treatment served as control. TGF-β1 increased nuclear staining for pSmad2, and this was almost completely blocked by tranilast. Photomicrographs were taken at × 400 magnification. Four experiments yielded similar results. (b) 4T1 cells were deprived of serum for 24 h followed by culture in complete medium in the presence or absence of vehicle (DMSO) or tranilast (800 μmol/l) for 24 h. The cells were lysed and analyzed for pSmad2 by western blotting. Upper panel: picture of the western blot; lower panel: densities of pSmad2 bands as percentage of β-actin controls. There is approximately 38% reduction in the level of pSmad2. This is one of the two experiments that yielded similar results. (c) 4T1 cells were grown in flat-bottom 96-well plates overnight, followed by serum deprivation for 24 h. After that, cells were cultured for another 24 h in complete medium in the presence of DMSO (control) or 800 μmol/l tranilast. The level of phosphorylated and total ERK1/2 and JNK were measured by CASE enzyme-linked immunosorbent assay, and the relative extent of phosphorylation was calculated, according to the supplier's protocol. The extent of phosphorylation refers to the proportion (fraction) of the total protein (ERK or JNK) that is phosphorylated. Results are the mean ± SD of three separate experiments. Tranilast significantly ($P < 0.05$) reduced the phosphorylation of both JNK and ERK1/2. We also examined phosporylation of ERK at earlier time points – 0, 30, 60, and 90 min. We saw phosphorylation of ERK1/2, but tranilast did not inhibit phosphorylation at these early time points.

800 μmol/l tranilast were 43 ± 2.9, 53 ± 2.9, 55 ± 2.9, and 42 ± 2.9 pg/ml (mean ± SD, $n = 3$, $P > 0.05$). Thus, the levels of TGF-β1 in the supernatants of 4T1 cells were not significantly reduced by tranilast (although immunoblots of proteins from cell lysates showed lower levels of TGF-β1; see below). Despite this constitutive production, the addition of active TGF-β1 (2 ng/ml) to the culture medium markedly enhanced the level of pSmad2 nuclear staining (Fig. 2a), which was inhibited by tranilast, consistent with a blockade of TGF-β signaling. We confirmed this further with western blot analysis of the cell lysates. As shown in Fig. 2b, tranilast treatment reduced the pSmad2 level as compared with the control cells (same medium with no tranilast).

Effect of tranilast on the phosphorylation of extracellularly regulated kinase 1 and 2 and JNK

ERK1/2, p38, and JNK are activated by serum, growth factors and cytokines (including TGF-β) [32]. ERK1/2 is aberrantly regulated in many cancer cells [32–34]. ERK, p38, and JNK have been implicated in TGF-β-dependent EMT and tumor cell migration [35,36]. Thus, we examined whether tranilast can depress phosphorylation

Fig. 3

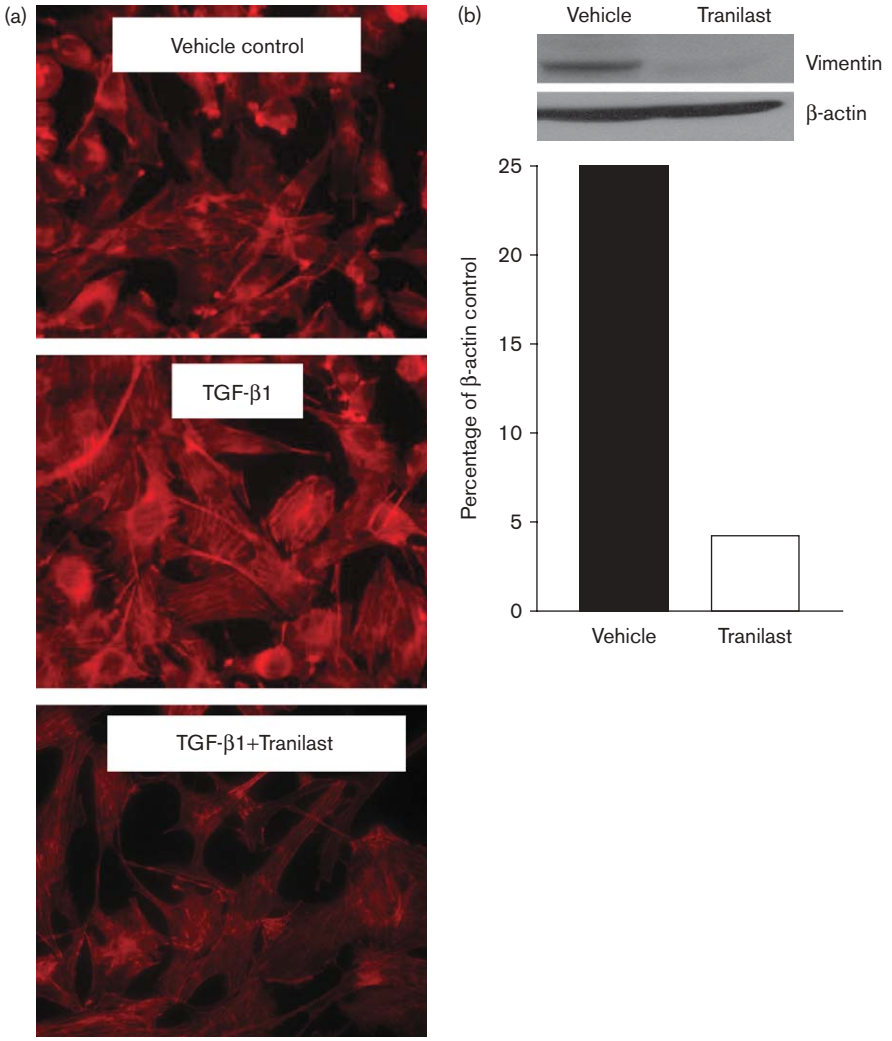

Tranilast inhibits TGF-β1-induced epithelial-to-mesenchymal transition (EMT) in 4T1 cells. (a) 4T1 cells were attached to cover slips and cultured for 48 h in the presence and absence of tranilast (800 μmol/l) and TGF-β1 (2 ng/ml). The cells were stained for F-actin with Alexa Fluor 568-conjugated phalloidin. Photographs were taken at a magnification of × 400. Addition of TGF-β1 to the cultures induced EMT as revealed from massive F-actin fiber organization and this was markedly reduced by tranilast treatment. Four experiments yielded similar results. Tranilast also inhibited EMT at a concentration of 200 μmol/l, but the effect was less marked (data not shown). (b) 4T1 cells were deprived of serum for 24 h followed by culture in complete medium in the presence or absence of vehicle (dimethyl sulfoxide) or tranilast (800 μmol/l) for 48 h. The cells were lysed and analyzed for vimentin (mesenchymal marker) by western blot as in Materials and methods. Upper panel: picture of the western blot; lower panel: densities of vimentin bands as percentage of β-actin controls. Tranilast treatment drastically reduced the vimentin level. Two experiments yielded similar results.

of these kinases in 4T1 cells. As expected, serum induced phosphorylation of ERK1/2 and JNK, and in both cases this was significantly reduced by tranilast (Fig. 2c) as determined by a CASE cellular ELISA. However, serum-induced phosphorylation of p38 was not affected by tranilast (data not shown).

Tranilast inhibits epithelial-to-mesenchymal transition of 4T1 cells

We investigated whether tranilast treatment can inhibit EMT in 4T1 cells in culture. As this cell line produces TGF-β1, the untreated cells had a mixture of both epithelial and mesenchymal-type cells (Fig. 3a), indicating EMT of some cells. This basal level of EMT was inhibited by either tranilast or an anti-TGF-β monoclonal antibody (data not shown). The cells incubated for 48 h with TGF-β1 (2 ng/ml) showed a markedly increased level of EMT, as indicated by the large amount of organized F-actin fibers (Fig. 3a). Tranilast inhibited the TGF-β1-induced EMT, as indicated by the reduced number of mesenchymal-type cells and the reduced level of organized F-actin (Fig. 3a). To corroborate this further, we analyzed the levels of vimentin, a mesenchymal marker, by western blot analysis. As shown in Fig. 3b, tranilast drastically reduced the vimentin level in 4T1 cells, as compared with the control.

Inhibition of cytokine production by lymphoid cells and 4T1 cells

In these experiments we isolated total murine spleen cells, and in some cases we isolated the splenic CD4+CD25– and CD8+ T cell subpopulations. T cells, or unfractionated spleen cells, were stimulated *in vitro* with CD3/CD28 mAbs. CD3/CD28 stimulation induces the production of several cytokines by T cells, including TGF-β1, interferon-γ, IL-10, and IL-17. In addition, we incubated the spleen cells with LPS, which acts on other (non-T) spleen cells and induces production of IL-6. Cytokine levels were measured by ELISA. We found that tranilast strongly inhibited the production of TGF-β1 by both CD4+CD25– (conventional Th-type cells) and CD8+ cells (cytotoxic T lymphocytes) (Fig. 4a). Indeed, ≥ 50% suppression was observed at tranilast concentration of 50 μmol/l. In the case of cultured 4T1 tumor cells, as noted previously, tranilast (at 50–800 μmol/l) did not significantly reduce the levels of TGF-β1 in culture supernatants. This suggested that tranilast did not act on 4T1 cells, unlike lymphocytes, by suppressing the production of TGF-β. These levels were, however, measured after 24 h in culture and it is possible that levels peak, which might mask a moderate reduction in cytokine production. Indeed, at 24 h, immunoblots of proteins from 4T1 whole-cell lysates revealed an approximately 54% reduction in TGF-β1 expression with

Fig. 4

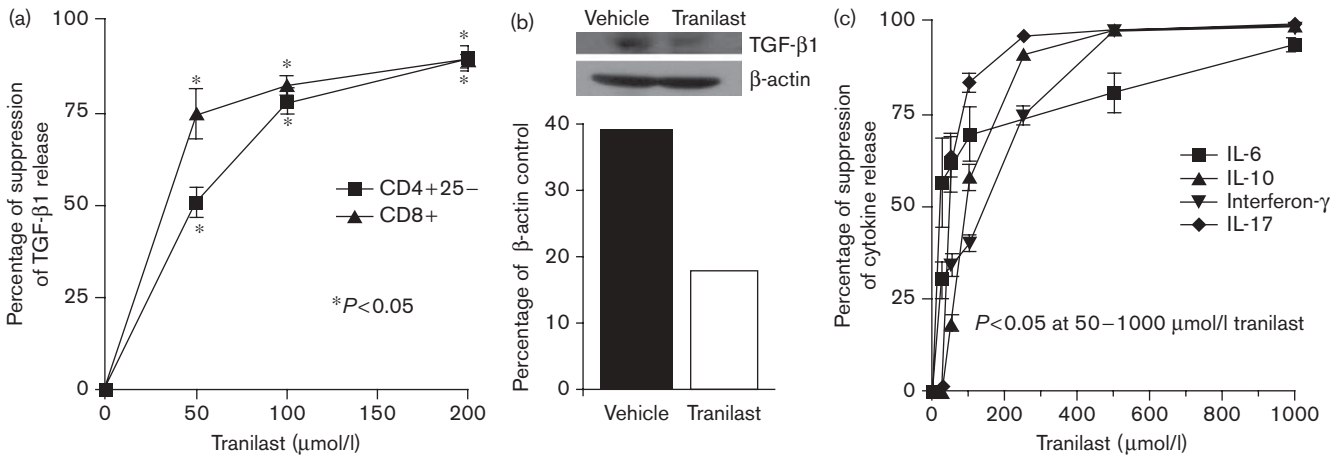

Effect of tranilast on cytokine release/production by spleen cells and 4T1 cell. (a) CD4+25– and CD8+ T cells were isolated from C57BL/6 mice and stimulated with plate-bound anti-CD3 and anti-CD28 mAbs, in the presence or absence of tranilast for 48 h. Then the supernatant was acidified for TGF-β1 activation, and TGF-β1 levels in the culture supernatant were measured by enzyme-linked immunosorbent assay. The control T cells (without tranilast) generated TGF-β1 levels of 83 ± 8.7 pg/ml in CD4+ cells and 39 ± 5.2 pg/ml in CD8+ T cells (mean ± SD; $n=3$). At all concentrations, tranilast significantly inhibited the production of TGF-β1 by both cell types ($P<0.05$). (b) 4T1 cells were deprived of serum for 24 h followed by culture in complete medium in the presence or absence of vehicle (dimethyl sulfoxide) or tranilast (800 μmol/l) for 24 h. The cells were lysed and analyzed for TGF-β1 by immunoblotting. The size of the unprocessed TGF-β1 precursor peptide is approximately 48 kDa. Upper panel: picture of the immunoblot; lower panel: densities of TGF-β1 bands as percentage of β-actin controls. There is approximately 54% tranilast-induced reduction in the expression level of TGF-β1. This is a representative experiment of two experiments. (c) Splenocytes were stimulated with plate-bound anti-CD3 and anti-CD28 mAbs in the presence or absence of tranilast. At 48 h, IL-10, interferon-γ, and IL-17 in the culture supernatants were measured. Alternatively, in some wells, the production of IL-6 was stimulated by lipopolysaccharide (LPS). Tranilast significantly ($P<0.05$) inhibited the secretion of all these cytokines at concentrations similar to those that inhibited TGF-β1 production by T cells. The control-stimulated levels of IL-6, IL-10, interferon-γ, and IL-17 were 13 ± 3.5, 723 ± 33, 1200 ± 199, and 476 ± 24 pg/ml (mean ± SD, $n=3$), respectively. For both (a) and (b), two experiments yielded similar results.

tranilast, detected primarily as the unprocessed precursor peptide (Fig. 4b). Similarly, in-vivo tranilast treatment resulted in a 40–50% reduction in the levels of the TGF-β propeptide in protein extracts of transplanted 4T1 tumors (data not shown). This suggests that tranilast suppresses the production of TGF-β by 4T1 cells at least partially.

The effects of tranilast were not limited to TGF-β production. In CD3/CD28-stimulated or LPS-stimulated spleen cells, tranilast also inhibited the production of IL-6, IL-10, IL-17, and interferon-γ, at concentrations in the same range as those that inhibited TGF-β1 (Fig. 4c). When we examined the supernatants of 4T1 cells for these cytokines, they were either present in low amounts or undetectable, and we could not establish whether or not tranilast was suppressive (data not shown).

Tranilast inhibits the growth and metastasis of transplanted 4T1 cells

Administration of tranilast by gavage markedly inhibited the growth of 4T1 cells transplanted in the mammary fat pad of female BALB/c mice, as indicated by the significant reduction in primary tumor volumes (approximately 50%) (Fig. 5). Tranilast treatment also dramatically reduced metastasis of tumor to the lungs. As shown in Fig. 6a, the lungs of mice in the vehicle-treated groups have about 12 times more metastatic tumors as compared with the tranilast-treated group. Furthermore, the metastatic lung tumors of vehicle-treated mice were considerably larger than those of the tranilast group (Fig. 6b and c). In the liver (Fig. 6d), we found a maximum of two metastatic tumors per liver section in vehicle-treated mice. However, although about 60% of vehicle-treated mice developed liver metastases, no metastases were detected in the liver of tranilast-treated mice.

Fig. 5

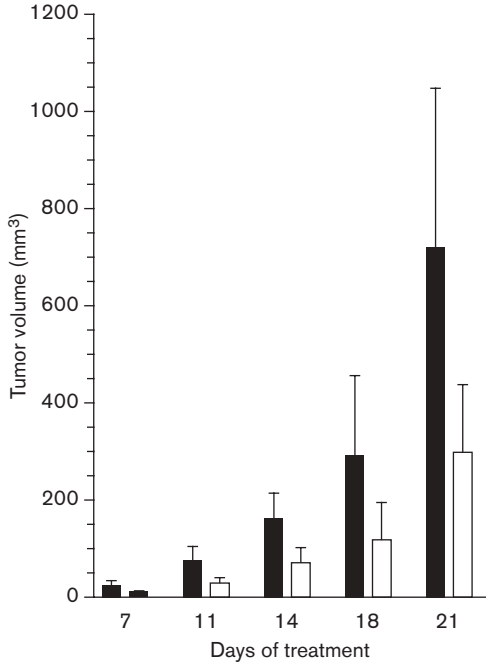

Tranilast inhibits the growth of transplanted 4T1 mammary carcinoma. 4T1 cells were transplanted orthotopically in mammary fat pads of 6-week-old female BALB/c mice (eight mice in each group). Tranilast was administered by gavage at a dose of 300 mg/kg body weight from day 0 (day of cancer cell transplantation) to the end of the treatment. Tumor volume (mean ± SD, $n=8$) over time is reported (■, vehicle group; □, tranilast group). At all time points, tumor size in the tranilast group was significantly lower than in the vehicle group ($P<0.05$). Three experiments yielded similar results.

Discussion

We found that tranilast inhibits the proliferation of all the tumor cell lines we tested, that is, the MDA-MB-231 and MCF-7 human breast carcinoma cell lines, the 4T1 mouse mammary carcinoma, the LA7 rat mammary carcinoma (reported to have cancer stem cell properties) [26], as well as mouse LLC (lung carcinoma), and EL-4 (thymoma). This occurred without apparent cytotoxicity, and tranilast seemed to arrest cell cycle at the S-phase at a moderate concentration (200 μmol/l) and at the G1-phase at a higher concentration (800 μmol/l). The mechanism by which tranilast blocks cell cycling remains to be fully elucidated. This could be related to reduced ERK activation (see below), which is normally sensitive to TGF-β [35,36] and several other stimuli. Furthermore, previous studies showed that tranilast induces the cyclin-dependent kinase inhibitor $p21^{WAF1}$ and the tumor suppressor p53 [37].

As our primary goal was to study metastatic disease, we focused on the highly metastatic 4T1 cell line. Consistent with its known anti-TGF-β effects, tranilast blocked TGF-β signaling as manifested by reduced nuclear pSmad2. Interestingly, tranilast did not prevent TGF-β1 secretion by 4T1 cells, although it strongly inhibited TGF-β1 production by T cells (see below). However, in the case of 4T1 cells, culture supernatant levels might not accurately reflect total TGF-β production over time. This is suggested by the finding that immunoblots of proteins extracted from cultured 4T1 cells showed an approximately 50% reduction in the TGF-β precursor peptide (the main form identified in the cytoplasm) in the presence of tranilast. A similar degree of tranilast-mediated suppression was also noted *in vivo* in transplanted 4T1 tumors (data not shown). We have not established whether this degree of suppression is sufficient to alter tumor progression, but we speculate that it is. Tranilast also inhibited ERK1/2 and JNK phosphorylation, and suppressed EMT. Importantly, we report that tranilast inhibits the growth of orthotopically transplanted 4T1 cells by more than 50%. Its effects on lung and liver metastases, however, were even more impressive with over 90% reduction in the lungs.

Fig. 6

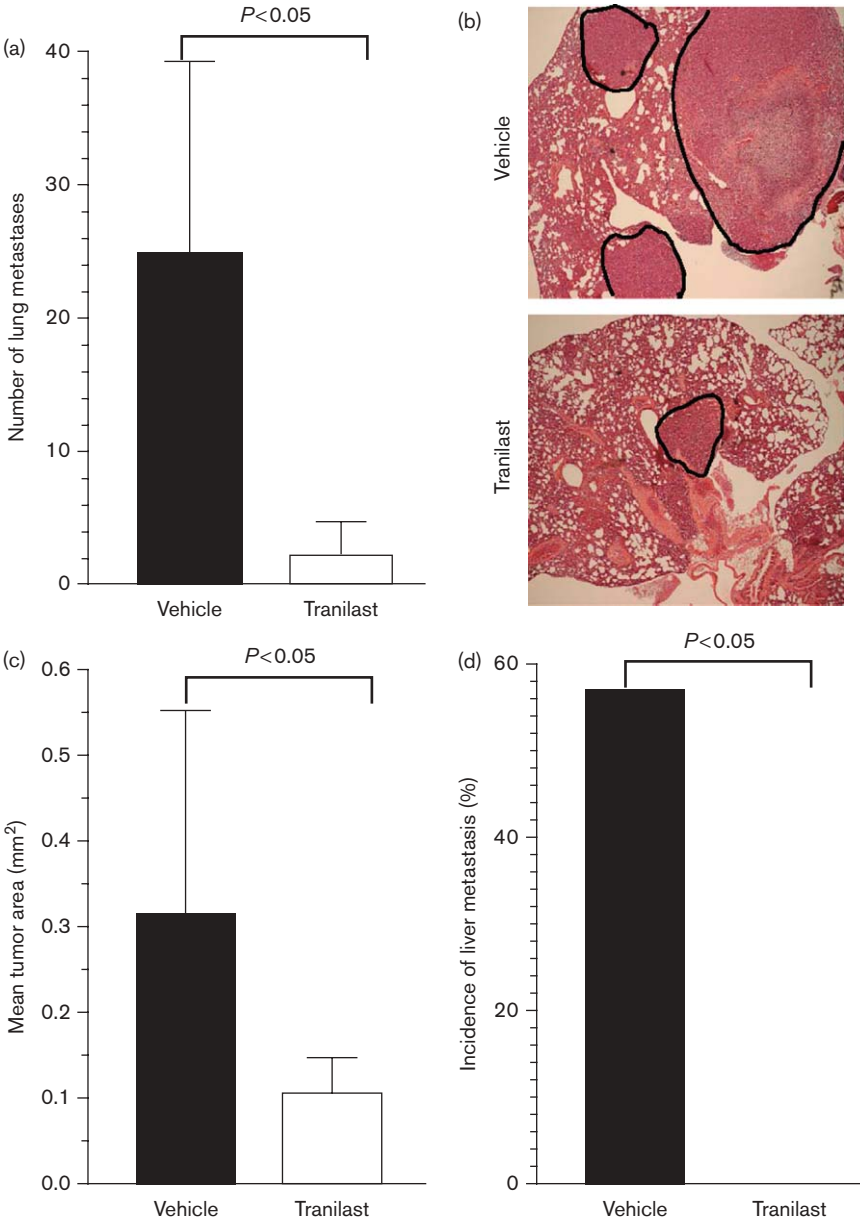

Tranilast inhibits metastasis of 4T1 mammary carcinoma to the lungs and liver. Mice were transplanted with 4T1 cells and treated with tranilast by gavage, as in Fig. 5 (eight mice in each group). On day 28 of treatment, the mice were killed and the lungs and liver were collected and examined histologically. (a) Number of tumors per lung section (■, vehicle; □, tranilast), expressed as the mean ± SD ($n=8$). (b) Histological sections of lungs showing metastatic tumors. As shown here, the tranilast-treated mice had smaller tumors than the vehicle-treated group (marked areas). (c) The area of each metastatic tumor lesions was measured in each lung section by a morphometric method. The mean area per metastatic tumor was significantly higher in the vehicle group than in the tranilast group ($P<0.05$). (d) Incidence of metastasis to liver (■, vehicle; □, tranilast). Unlike the vehicle-treated group, the tranilast-treated group had no metastases ($P<0.05$). The photomicrographs were taken at a magnification of ×40. Three experiments yielded similar results.

Indeed, unlike control mice, tranilast-treated mice only developed a few small lung metastases and no liver metastases at all.

The ability of tranilast to inhibit TGF-β signaling is probably a major contributor to its antimetastatic effects. TGF-β plays a major role in cancer by suppressing tumor growth in the early phase, but promoting tumor metastasis at later stages (reviewed in Ref. [9]). Indeed, LAP-TGF-β (the latent form) is frequently produced by cancer cells, and it seems that these cells can activate this cytokine, possibly by several mechanisms [9]. Recently, we have identified neuropilin-1 as a molecule expressed by cancer cells (including 4T1), which can activate TGF-β

[38]. TGF-β signaling depends on both Smad and non-Smad pathways [9]. As tranilast inhibited the accumulation of pSmad2, we postulate that it inhibits signaling at an early point (yet to be identified) in the Smad pathway.

With tumor progression, TGF-β becomes a tumor promoter and induces EMT by Smad-dependent and independent pathways [39–41]. Indeed, TGF-β has been shown to activate at least two different MAPK pathways, that is, ERK and JNK [35,36,41], relevant to tumor progression. Notably, the ERK1/2 signaling pathway is important for the growth of normal and cancer cells [32–34]. Our study reveals that tranilast reduces ERK1/2 phosphorylation, and this could be a key mechanism by which it inhibits tumor cell growth. Indeed, ERK1/2 is considered as a master regulator of G1-S phase transition [42]. Furthermore, our finding that tranilast also inhibits JNK activation points to a more general blockade of these pathways. The combined inhibition of ERK and JNK phosphorylation may explain the ability of tranilast to block EMT and metastasis. TGF-β signaling and ERK1/2 phosphorylation have been linked to tumor cell migration [35,36], and we recently observed that tranilast significantly inhibits the migration of 4T1 cells for up to 96 h in an in-vitro wound assay (Subramaniam *et al.*, in preparation). Migration is an important step in metastasis, and this further supports our hypothesis that tranilast protects against metastatic disease.

Tranilast might act in the tumor microenvironment by suppressing TGF-β production by tumor cells and/or other cell types, such as lymphocytes, macrophages, and other lymphoid cells. We tested the ability of tranilast to suppress several cytokines *in vitro*. In purified CD+CD25− and CD8+ T cell populations stimulated with CD3/CD28 mAbs, tranilast strongly suppressed TGF-β1 secretion. Indeed, $\geq 50\%$ inhibition was observed at doses of 50 μmol/l, suggesting that T cells are more sensitive to the inhibitory effects of tranilast than the tumor cell lines we examined. Furthermore, stimulation of spleen cells (containing both T cells and other cell types) with either CD3/CD28 mAbs or LPS revealed that tranilast could suppress the production of interferon-γ, IL-6, IL-10, and IL-17. Although interferon-γ generally has a protective role against cancer, the other cytokines have all been linked to tumor progression [43–46]. The ability of tranilast to suppress these multiple cytokines could have profound effects on the development of antitumor immunity, tumor cell growth, and might also alter the tumor stroma.

Several large and small-molecular-weight drugs inhibiting TGF-β are being tested in preclinical and clinical trial for the therapy of fibrosis or cancer. This includes mAbs, soluble TGF-β receptors, antisense ODNs, and several inhibitors of ALK5 (TGF-βRI), as we have reviewed [9]. Most of these drugs are either at a preclinical or early clinical stage of development. In contrast, there is a long clinical experience with tranilast, and considerable evidence that it is well tolerated by patients. Indeed, the toxicity of tranilast is low, with an LD50 of greater than 1 g/kg in rats [47]. For the therapy of allergic and fibrotic diseases, tranilast is usually administered at a dose of 300 mg/day (in three divided doses), but in some clinical trials it has been administered at doses of 600–900 mg/day [47,48]. At the higher doses, approximately 11% of patients have experienced liver test abnormalities, which are reversible after withdrawal of the drug. Peak plasma levels of 100–200 μmol/l have been reported after the administration of a single dose of tranilast in the therapeutic range to humans [49]. With continuous administration of 600 mg/day dose, plasma concentrations ranged from 30 to 300 μmol/l [50]. These in-vivo levels correspond to concentrations of tranilast that reduced the proliferation of four out of six tumor cell lines we tested *in vitro*, and are clearly sufficient to inhibit the production of several cytokines (including TGF-β and IL-17) by lymphoid cells.

In addition to inhibiting TGF-β production and/or action, tranilast exerts other anticancer effects and, therefore, may have advantages over more specific TGF-β inhibitors. Our results suggest that tranilast has the potential of becoming a novel drug in the prevention of metastatic cancer. Remarkably, compared with recent reports, tranilast monotherapy seems to be more effective in preventing metastatic disease in the 4T1 model than either anti-TGF-β monotherapy with the 1D11 antibody [51], paclitaxel monotherapy [52], or paclitaxel combined with endostatin gene therapy [52]. Moreover, the ability of tranilast to inhibit 4T1 primary tumor growth appears comparable with either paclitaxel or doxorubicin [52,53].

In conclusion, tranilast inhibited the proliferation of human, mouse, and rat mammary carcinoma cell lines. It inhibited Smad-dependent, ERK, and JNK signaling pathways, as well as EMT. Tranilast also inhibited the production of several cytokines by immune cells, including TGF-β and IL-17 that have been linked to cancer progression. *In vivo*, it significantly inhibited the growth of 4T1 mouse mammary carcinoma, and was highly effective in preventing metastatic disease. Thus, tranilast has potential activity as an antimetastatic agent in breast cancer.

Acknowledgements

The authors acknowledge the valuable help from Dr Yelena Glinka. This work has been supported by the Ontario Institute for Cancer Research of the province of Ontario (Canada), the Krembil Foundation (Toronto, Canada), and the Li Ka Shing Knowledge Institute and

Keenan Research Centre of St Michael's Hospital, Toronto, Ontario, Canada.

Competing interest: none declared.

References

1 Moulder S, Hortobagyi GN. Advances in the treatment of breast cancer. *Clin Pharmacol Ther* 2008; **83**:26–36.
2 Azuma H, Banno K, Yoshimura T. Pharmacological properties of N-(dimethoxycinnamonyl) anthranilic acid (N-5′), a new anti-atopic agent. *Br J Pharmacol* 1976; **58**:483–488.
3 Konneh M. Tranilast, Kissei Pharmaceuticals. *Idrugs* 1998; **1**:141–146.
4 Koda A, Kurashina Y, Nakazawa M. The inhibition mechanism of histamine release by N-(3′, 4′-dimethoxycinnamonyl) anthranilic acid. *Int Arch Aller Appl Immunol* 1985; **77**:244–245.
5 Komatsu H, Kojima M, Tsutsumi N. Study of the mechanism of inhibitory action of tranilast on chemical mediator release. *Jpn J Pharmacol* 1988; **46**:43–51.
6 Suzawa H, Kikuchi S, Arai N, Koda A. The mechanism involved in the inhibitory action of tranilast on collagen biosynthesis of keloid fibroblasts. *Jpn J Pharmacol* 1992; **60**:91–96.
7 Fukayama J, Miyazawa K, Hamano S, Ujiie A. Inhibitory effect of tranilast on proliferation, migration and collagen synthesis of human vascular smooth muscle cells. *Can J Physiol Pharmacol* 1996; **74**:80–84.
8 Yamada H, Tajima S, Nshikawa T, Murad S, Pinnell SR. Tranilast a selective inhibitor of collagen synthesis in human skin fibroblasts. *J Biochem* 1994; **116**:892–897.
9 Prud'homme GJ. Pathobiology of transforming growth factor beta in cancer, fibrosis and immunologic disease, and therapeutic considerations. *Lab Invest* 2007; **87**:1077–1091.
10 Jones SE, Gilbert RE, Kelly DJ. Tranilast reduces mesenteric vascular collagen deposition and chymase-positive mast cells in experimental diabetes. *J Diabet Complic* 2004; **18**:309–315.
11 Bonnet F, Cao Z, Cooper ME, Cox AJ, Kelly DJ, Gilbert RE. Tranilast attenuates vascular hypertrophy, matrix accumulation and growth factor overexpression in experimental diabetes. *Diabetes Metab* 2003; **29** (**4 Pt 1**):386–392.
12 Kelly DJ, Zhang Y, Gow R, Gilbert RE. Tranilast attenuates structural and functional aspects of renal injury in the remnant kidney model. *J Am Soc Nephrol* 2004; **15**:2619–2629.
13 Qi W, Chen X, Twigg S, Polhill TS, Gilbert RE, Pollock CA. Tranilast attenuates connective tissue growth factor-induced extracellular matrix accumulation in renal cells. *Kidney Int* 2006; **69**:989–995.
14 Kelly DJ, Zhang Y, Cox AJ. Combination therapy with tranilast and angiotensin-converting enzyme inhibition provides additional renoprotection in the remnant kidney model. *Kidney Int* 2006; **69**:1954–1960.
15 Platten M, Wild-Bode C, Wick W, Leitlein J, Dichgans J, Weller M. N-(3′, 4′-dimethoxycinnamonyl) anthranilic acid (tranilast) transforming growth factor-β release and reduces migration and invasiveness of human malignant glioma cells. *Int J Cancer* 2001; **93**:53–61.
16 Hirori M, Onda M, Uchida E, Aimoto T. Anti-tumor effect of N-(3′, 4′-dimethoxycinnamonyl) anthranilic acid (tranilast) on experimental pancreatic cancer. *J Nippon Med Sch* 2002; **69**:224–234.
17 Shime H, Kariya M, Orii A. Tranilast inhibits the proliferation of uterine leiomyoma cells in vitro through G1 arrest associated with the induction of $p21^{waf1}$ and p^{53}. *J Clin Endocrino Metab* 2002; **87**:5610–5617.
18 Noguchi N, Kawashiri S, Tanak A. Effect of fibroblast growth inhibitor on proliferation and metastasis of oral squamous cell carcinoma. *Oran Oncol* 2003; **39**:240–247.
19 Bandyopadhyay A, Agyin JK, Wang L, Tang Y, Lei X, Story BM, *et al*. Inhibition of pulmonary and skeletal metastasis by transforming growth factor-β type I receptor kinase inhibitor. *Cancer Res* 2006; **66**:6714–6721.
20 Ge R, Rajeev V, Ray P, Lattime E, Rittling S, Medicherla S, *et al*. Inhibition of growth and metastasis of mouse mammary carcinoma by selective inhibitor of transforming growth factor-β type I receptor kinase in vivo. *Clin Cancer Res* 2006; **12**:4315–4330.
21 McEarchern JA, Kobie JJ, Mack V, Wu RS, Meade-Tollin L, Arteaga CL, *et al*. Invasion and metastasis of a mammary tumor involves TGF-β signaling. *Int J Cancer* 2001; **91**:76–82.
22 Yin JJ, Selander K, Chirgwin JM. TGF-β signaling blockade inhibits PTHrP secretion by breast cancer cells and bone metastasis development. *J Clin Invest* 1999; **103**:197–206.
23 Iyer S, Wang ZG, Akhtari M, Zhao W, Seth P. Targeting TGF beta signaling for cancer therapy. *Cancer Biol Ther* 2005; **4**:261–266.
24 Lahn M, Kloeker S, Berry BS. TGF-beta inhibitors for the treatment of cancer. *Expert Opin Invest Drugs* 2005; **14**:629–643.
25 Pulaski BA, Ostrand-Rosenberg S. Reduction of established spontaneous mammary carcinoma metastases following immunotherapy with major histocompatibility complex class II and B7.1 cell-based tumor vaccines. *Cancer Res* 1998; **58**:1486–1493.
26 Zucchi I, Sanzone S, Astigiano S. The properties of a mammary gland cancer stem cell. *Proc Natl Acad Sci U S A* 2007; **104**:10476–10481.
27 Chakrabarti R, Zhou ZF, Chang Y. A mutant B7-1/Ig fusion protein that selectively binds to CTLA-4 ameliorates anti-tumor DNA vaccination and counters regulatory T cell activity. *Vaccine* 2005; **23**:4553–4564.
28 Glinka Y, Chang Y, Prud'homme GJ. Protective regulatory T cell generation in autoimmune diabetes by DNA covaccination with islet antigens and a selective CTLA-4 ligand. *Mol Ther* 2006; **14**:578–587.
29 Beshay E, Croze F, Prud'homme GJ. The phosphodiesterase inhibitors pentoxifylline and rolipram suppress macrophage activation and nitric oxide production in vitro and in vivo. *Clin Immunol* 2001; **98**:272–279.
30 Scholzen T, Gerdes J. The ki-67 protein: from the known to the unknown. *J Cell Physiol* 2000; **182**:311–322.
31 Schmierer B, Hill CS. TGFbeta-SMAD signal transduction: molecular specificity and functional flexibility. *Nat Rev* 2007; **8**:970–982.
32 Pearson G, Robinson F, Beers T, Xu B, Karandikar M, Berman K, *et al*. Mitogen-activated protein kinase pathways: regulation and physiological functions. *Endocrine Rev* 2001; **22**:153–183.
33 Lev DC, Kim LS, Melnikov V, Ruiz M, Ananthaswamy HN, Price JE. Dual blockade of EGFR and ERK1/2 phosphorylation potentiates growth inhibition of breast cancer cells. *Br J Cancer* 2004; **91**:795–802.
34 Steinmetz R, Wagoner HA, Zeng P, Hammond JR, Hannon TS, Meyers JL, *et al*. Mechanisms regulating the constitutive activation of the extracellular signal-regulated kinase (ERK) signaling pathway in ovarian cancer and the effect of ribonucleic acid interference for ERK1/2 on cancer cell proliferation. *Mol Endocrinol* 2004; **18**:2570–2582.
35 Giehl K, Imamichi Y, Menke A. Smad4-independent TGF-b signaling in tumor cell migration. *Cell Tissues Organs* 2007; **185**:123–130.
36 Zhang YE. Non-Smad TGF-β signaling pathways. In: Derynck R, Miyazono K, editors. *The TGF-β family*. New York: Cold Spring Harbor Laboratory Press; 2008. pp. 419–438.
37 Shime H, Kariya M, Orii A, Momma C, Kanamori T, Fukuhara K, *et al*. Tranilast inhibits the proliferation of uterine leiomyoma cells in vitro through G1 arrest associated with the induction of p21(waf1) and p53. *J Clin Endocrinol Metab* 2002; **87**:5610–5617.
38 Glinka Y, Prud'homme GJ. Neuropilin-1 is a receptor for transforming growth factor β-1, activates its latent form, and promotes regulatory T cell activity. *J Leuko Biol* 2008; **84**:302–310.
39 Zavadil J, Bottinger E. TGF-beta and epithelial-to-mesenchymal transitions. *Oncogene* 2005; **24**:5764–5774.
40 Han G, Lu SL, Li AG, He W, Corless CL, Kulesz-Martin M, *et al*. Distinct mechanisms of TGF-beta1-mediated epithelial-to-mesenchymal transition and metastasis during skin carcinogenesis. *J Clin Invest* 2005; **115**:1714–1723.
41 Xie L, Law BK, Chytil AM, Brown KA, Aakre M, Moses HL. Activation of the Erk pathway is required for TGF-beta1-induced EMT in vitro. *Neoplasia* 2004; **6**:603–610.
42 Meloche S, Pouyssegur J. The ERK1/2 mitogen-activated protein kinase pathway as the master regulator of G1 to S-phase transition. *Oncogene* 2007; **26**:3227–3239.
43 Nicolini A, Carpi A, Rossi G. Cytokines in breast cancer. *Cytokine Growth Factor Rev* 2006; **17**:325–337.
44 Wilczynski JR, Radwan M, Kalinka J. The characterization and role of regulatory T cells in immune reactions. *Front Biosci* 2008; **13**:2266–2274.
45 Bettelli E, Carrier Y, Gao W, Korn T, Strom TB, Oukka M, *et al*. Reciprocal developmental pathways for the generation of pathogenic effector TH17 and regulatory T cells. *Nature* 2006; **441**:235–238.
46 Nam JS, Terabe M, Kang MJ, Chae H, Voong N, Yang YA, *et al*. Transforming growth factor beta subverts the immune system into directly promoting tumor growth through interleukin-17. *Cancer Res* 2008; **68**:3915–3923.
47 Isaji M, Miyata H, Ajisawa Y. Tranilast: a new application in the cardiovascular field as an antiproliferative drugs. *Cardiovascular Drug Rev* 1998; **16**:288–299.
48 Holmes DR Jr, Savage M, LaBlanche JM, Grip L, Serruys PW, Fitzgerald P, *et al*. Results of prevention of restenosis with tranilast and its outcomes (PRESTO) trial. *Circulation* 2002; **106**:1243–1250.
49 Slobodzian DK, Hsieh JY, Bayne WE. Simultaneous determination of tranilast and metabolites in plasma and urine using high-performance liquid chromatography. *J Chromatogr* 1985; **345**:345–354.

50 Kusama H, Kikuchi S, Tazawa S, Katsuno K, Baba Y, Zhai YL, *et al*. Tranilast inhibits the proliferation of human coronary smooth muscle cell through the activation of $p21^{waf1}$. *Atherosclerosis* 1999; **143**:307–313.
51 Nam JS, Terabe M, Mamura M, Kang MJ, Chae H, Stuelten C, *et al*. An anti-transforming growth factor beta antibody suppresses metastasis via cooperative effects on multiple cell compartments. *Cancer Res* 2008; **68**:3835–3843.
52 Li J, Dong X, Xu Z, Jiang X, Jiang H, Krissansen GW, *et al*. Endostatin gene therapy enhances the efficacy of paclitaxel to suppress breast cancers and metastases in mice. *J Biomed Sci* 2008; **15**:99–109.
53 Du GJ, Song ZH, Lin HH, Han XF, Zhang S, Yang YM. Luteolin as a glycolysis inhibitor offers superior efficacy and lesser toxicity of doxorubicin in breast cancer cells. *Biochem Biophys Res Commun* 2008; **372**:497–502.